

N. Lu et al.: Delamination of stiff islands patterned on stretchable substrates

Nanshu Lu<sup>a</sup>, Juil Yoon<sup>a</sup>, Zhigang Suo<sup>a</sup>

<sup>a</sup>Harvard University, School of Engineering and Applied Science, Cambridge, MA, USA

# Delamination of stiff islands patterned on stretchable substrates

*Dedicated to Professor Dr. Wolfgang Pompe on the occasion of his 65<sup>th</sup> birthday*

In one design of flexible electronics, thin-film islands of a stiff material are fabricated on a polymeric substrate, and functional materials are grown on these islands. When the substrate is stretched, the deformation is mainly accommodated by the substrate, and the islands and functional materials experience relatively small strains. Experiments have shown that, however, for a given amount of stretch, the islands exceeding a certain size may delaminate from the substrate. We calculate the energy release rate using a combination of finite element and complex variable methods. Our results show that the energy release rate diminishes as the island size or substrate stiffness decreases. Consequently, the critical island size is large when the substrate is compliant. We also obtain an analytical expression for the energy release rate of debonding islands from a very compliant substrate.

**Keywords:** Flexible electronics; Island size; Delamination; Complex potential

## 1. Introduction

Flexible electronics are promising for diverse applications, such as rollable displays [1], conformal sensors, and printable solar cells [2]. These systems are thin, rugged, and lightweight. They can be manufactured at low cost, for example, by roll-to-roll printing. Flexible electronics usually consists of inorganic electronic materials fabricated on a compliant

polymer substrate [2–4]. The composite structure may experience one-time severe stretch during manufacture (e.g., retinal electronic prosthesis), or repeated modest bends and twists in service (e.g., rollable electronic reader [1]). While the polymer substrate may sustain large deformation, thin films of most electronic materials rupture at small strains, say 1–2 % [5–9]. How to build flexible electronics with inorganic electronic materials remains a significant challenge.

One possible solution is to fabricate functional islands of stiff materials on a polymer substrate [10–13]. Since the islands are much stiffer than the substrate, when such a composite structure is stretched, the substrate carries most of the deformation, but the islands experience little strain [10–13]. A large island may fail, however, by several mechanisms. For example, the strain in the island may exceed a critical value so that the island itself may crack [10]. As another example, the island may delaminate from the substrate [12]. Experiments have shown that while  $40 \times 40 \mu\text{m}^2 \text{SiN}_x$  square islands debond and slip against the Kapton substrate when the whole structure is under 5.6 % tensile strain [12],  $200 \times 200 \mu\text{m}^2$  diamond-like-carbon (DLC) islands on PDMS substrate remain intact even under 25 % tensile strain [13]. This phenomenon raises the inquiry of delamination conditions, and consequently the critical island size, below which the islands will not delaminate.

The plan of the paper is as follows: Section 2 provides available theories related to film/substrate debonding; Section 3 describes the computational model and shows how

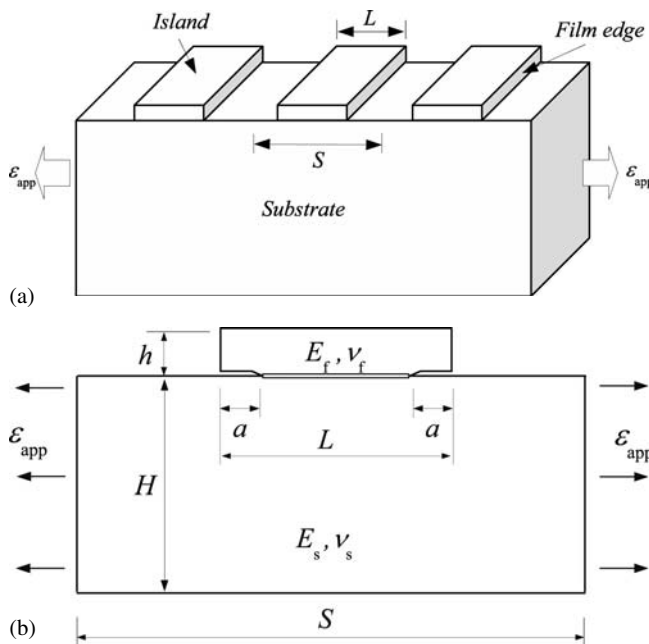


Fig. 1. (a) Schematics of an array of thin-film functional islands on compliant substrate, which is subject to uniaxial tensile strain  $\varepsilon_{app}$ . Subscript “f” denotes “film” and “s” means “substrate”.  $L$  is the island size and  $S$  is the island spacing. The thickness for film and substrate are  $h$  and  $H$  respectively. (b) Schematics of the plane strain model for one cell, where  $a$  is the crack size.

crack length, elastic mismatch and island size affect the energy release rate; Section 4 studies the critical island sizes. In the Appendix, we use the complex variable method to determine the energy release rate for debonding of a periodic array of islands from very compliant substrate.

## 2. Analytical results for film/substrate debonding

Figure 1a illustrates the structure to be studied. A periodic array of thin-film islands of a stiff material is patterned on a polymer substrate. When the substrate is stretched, part of the load is transferred to the islands through the shear stress on the interface at the edges of the islands [14]. This shear stress makes the islands susceptible to debonding. The period of the islands,  $S$ , sets the width of the unit cell in our calculation, as illustrated in Fig. 1b, with a single island, width  $L$  and thickness  $h$ . The thickness of the substrate is  $H$ . Both the film and the substrate are taken to be isotropic and linearly elastic, with Young’s modulus  $E$  and Poisson’s ratio  $\nu$  prescribed for each material, and subscripts f and s indicating the thin-film islands and the substrate. The two edges of the substrates are prescribed with displacements  $\pm\varepsilon_{app}S/2$ , and the nominal strain  $\varepsilon_{app}$  will be used to represent the applied load. A crack of length  $a$  emanates from either edge of the island. The structure is taken to deform under the plane strain conditions.

### 2.1. Steady state debonding

Hutchinson and Suo [15] considered a crack on the interface of two layers. Consider the case that the substrate is loaded uniformly along the edge with a certain tensile strain  $\varepsilon_{app}$ . When the tip of the crack is far away from the film edge, the crack attains a *steady state* and the energy release

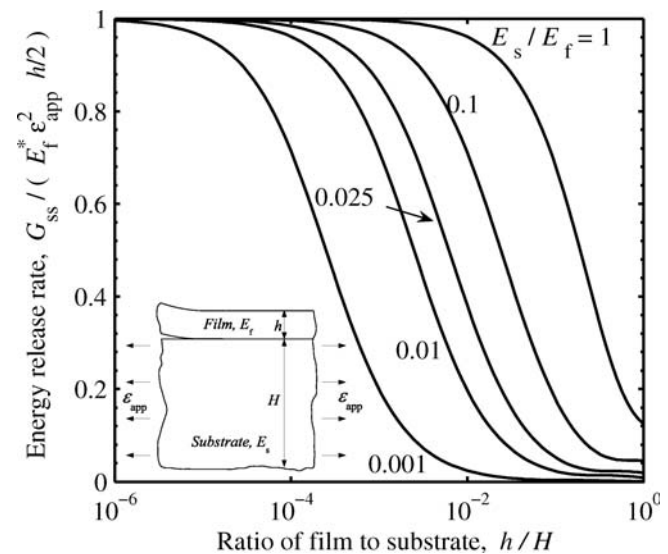


Fig. 2. Analytical result of steady state energy release rate as a function of thickness ratio and modulus ratio (Eq. (2)).

rate is independent of the crack length, given by

$$G_{ss} = \frac{E_f^* \varepsilon_{app}^2 h}{2} f(\Sigma, \eta) \quad (1)$$

with  $E^* = E/(1 - \nu^2)$  and

$$f(\Sigma, \eta) = \frac{\Sigma \eta^3 + 1}{\Sigma^2 \eta^4 + 4\Sigma \eta + 6\Sigma \eta^2 + 4\Sigma \eta^3 + 1} \quad (2)$$

where

$$\Sigma \equiv E_f^*/E_s^*, \quad \eta \equiv h/H$$

Figure 2 plots the normalized steady-state energy release rate as a function of  $h/H$  and  $E_s^*/E_f^*$ . For given thickness and modulus of the film, the energy release rate decreases when the thickness or the modulus of the substrate decreases. Two limiting cases are instructive:

(a) If the substrate is infinitely thick ( $H \rightarrow \infty$ ), namely  $\eta \rightarrow 0$ , obviously  $f(\Sigma, \eta) \rightarrow 1$  and Eq. (1) becomes

$$G_{ss} = \frac{E_f^* \varepsilon_{app}^2 h}{2} (\eta \rightarrow 0) \quad (3)$$

We use this value to normalize energy release rates for other configurations.

(b) If the film is rigid ( $E_f \rightarrow \infty$ ), namely  $\Sigma \rightarrow \infty$ , the role of film and substrate is reversed. The rigid film should be treated as an infinitely thick substrate and correspondingly the substrate is taken as a film with thickness  $H$  and Young’s modulus  $E_s$ . Consequently, the steady-state energy release rate is readily given by

$$G_{ss} = \frac{E_s^* \varepsilon_{app}^2 H}{2} (\Sigma \rightarrow 0) \quad (4)$$

### 2.2. Convergent debonding

With reference to Fig. 1b, when cracks from the two edges of an island approach each other, in the limit that the remaining bonded interface is short,  $L - 2a \ll h$ , both the

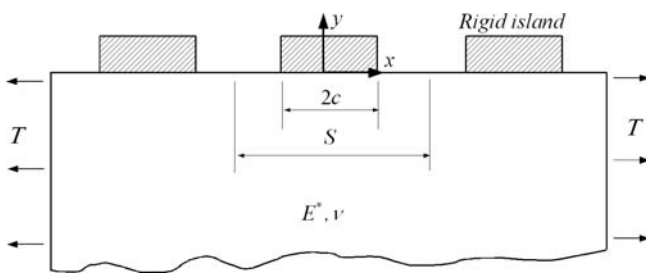


Fig. 3. Schematics of collinear periodic rigid islands on elastic solid under uniaxial tension.

film and the substrate can be viewed as half planes. The elasticity problem has been solved analytically, giving the energy release rate [16]

$$G = \frac{\pi}{16} \varepsilon_{\text{app}}^2 (L - 2a) \left( \frac{1}{E_s^*} + \frac{1}{E_f^*} \right)^{-1} \quad (5)$$

If the substrate is much more compliant than the island,  $E_s \ll E_f$ , the above result reduces to

$$G = \frac{\pi}{16} E_s^* \varepsilon_{\text{app}}^2 (L - 2a) \quad (6)$$

### 2.3. A periodic array of rigid islands

Figure 3 shows the limiting case  $E_s/E_f \rightarrow 0$ , which means the substrate is so compliant that the islands appear to be rigid. In this situation, the energy release rate is independent of the island thickness  $h$ , the island length  $L$  and the crack length, but depend on the bonded length  $2c = L - 2a$  and the island spacing. The boundary value problem of this limiting case is illustrated in Fig. 3, and solved analytically in Appendix, giving the energy release rate

$$G = \frac{E_f^* \varepsilon_{\text{app}}^2}{8} S \tan \frac{\pi(L - 2a)}{2S} \quad (7)$$

When the bonded length is small compared to the spacing between the islands, namely  $L - 2a \ll S$ , this result recovers Eq. (6).

## 3. Computational model and results

To examine how the above analytical expressions for limiting cases apply to stiff islands on a stretchable substrate, we use ABAQUS, a commercial finite element code, to calculate the energy release rate. Because of symmetry, only half of the unit cell in Fig. 1b is modeled. In calculations, we take  $v_f = v_s = 0.3$ ,  $H/h = 100$  and  $S/L = 1.5$ . Dimensional considerations dictate that the energy release rate should take the following form:

$$G = \frac{E_f^* \varepsilon_{\text{app}}^2 h}{2} g \left( \frac{a}{h}, \frac{E_s^* L}{E_f^* h} \right) \quad (8)$$

where  $g$  is a dimensionless function to be determined by using the finite element code.

Figure 4a plots the energy release rate as a function of the crack length at several values of  $E_s/E_f$ . The length of the island is fixed at  $L = 100h$ , and the length of the crack varies

from  $a = 0 - 50h$ . Everything else being fixed, we conclude that the more compliant the substrate, the smaller the energy release rate. This trend is understood as follows. If the stiffness of the substrate is comparable to that of the islands, the deformation in the substrate is rather uniform, leading to a maximum strain in the islands comparable to the applied strain, so that the reduction in elastic energy is large as the crack advances. By contrast, if the substrate is compliant, the applied strain is mainly accommodated by the portion of the substrate in between the stiff islands, while the strain in the islands is negligible, so that the energy release rate is small.

When the substrate is as stiff as the film,  $E_s/E_f = 1$ , the crack reaches the steady-state energy release rate  $G_{\text{ss}}$  when  $a/h \sim 1$ , and essentially maintains  $G_{\text{ss}}$  until the tip of the crack approaches that from the other edge of the island. When the substrate is more compliant than the film, however, the steady state is never reached. Instead, as the crack length increases, the energy release rate rises steeply to a peak at small crack length ( $a/h < 1$ ), and then decreases. Convergent debonding is also evident in Fig. 4a, in which Eq. (5) is plotted as dashed lines. These behaviors should

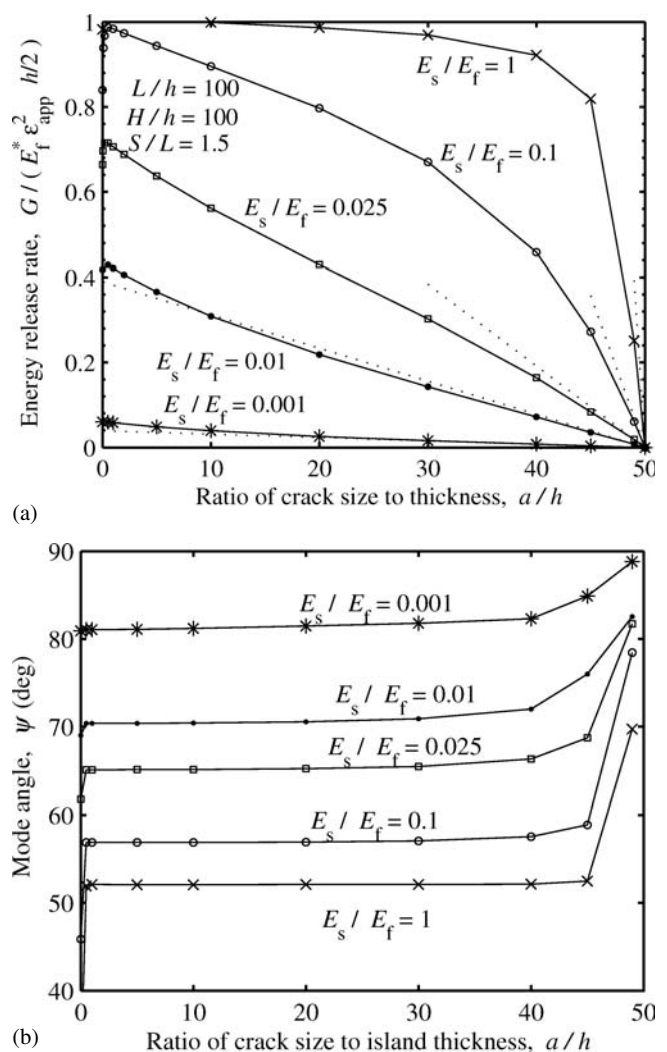


Fig. 4. FEM results of (a) energy release rate of debonding and (b) mode angle  $\psi$ , as functions of crack size  $a/h$  for elastic mismatch  $E_s/E_f$  from 0.001 to 1, with island size  $L/h$ , island spacing  $S/L$  and substrate thickness  $H/h$  fixed. The energy release rates for convergent debonding (Eq. (5)) are shown by dashed lines.

be compared with those described in [14, 17], where initial rising and convergent debonding were studied separately.

The mode angle of the interface crack is defined by the ratio of the mode II and mode I stress intensity factors:

$$\tan \psi = \frac{K_{II}}{K_I} \quad (9)$$

(Here we neglect the small effect of the oscillatory singularity; see Appendix.) Figure 4b shows that the mode angle can reach steady-state values, which are within 10% relative deviation compared with those calculated in [15]. The crack is progressively shear-dominated as the substrate becomes more compliant and as the crack becomes longer.

Figure 5 compares the calculated energy release rates with Eq. (7). When the substrate is very compliant,  $E_s/E_f = 0.001$ , Eq. (7) fits the calculated values well for the entire range of the crack length, indicating that in this case the islands are stiff enough to be viewed as being rigid. Equation (7) is also a fair approximation when the substrate is less compliant and the crack is long.

Figure 6 plots the energy release rate and the mode angle as a function of the crack length at several values of island lengths. The ratio of elastic moduli is fixed at  $E_s/E_f = 0.025$ , corresponding to, say  $E_f = 200$  GPa (a ceramic) and  $E_s = 5$  GPa (a polyimide). The energy release rate decreases as the island size decreases. From Fig. 6a we know that the smaller island, the lower energy release rate level. This trend is due to that the strain level in the island is small as the island reduces in size [18].

Also evident in Fig. 6a is that the energy release rate decreases with increasing crack length  $a$  at similar slopes for different island sizes. This slope is approximately predicted by the solution of convergent debonding, Eq. (5), which is plotted as dashed lines. However, using this slope to predict the maximum energy release rate is unreliable, particularly when the island is large. Figure 6b suggests that the steady-state value of mode angle is insensitive to the island size  $L$ , unless the island is too small for the crack to attain the steady-state mode angle.

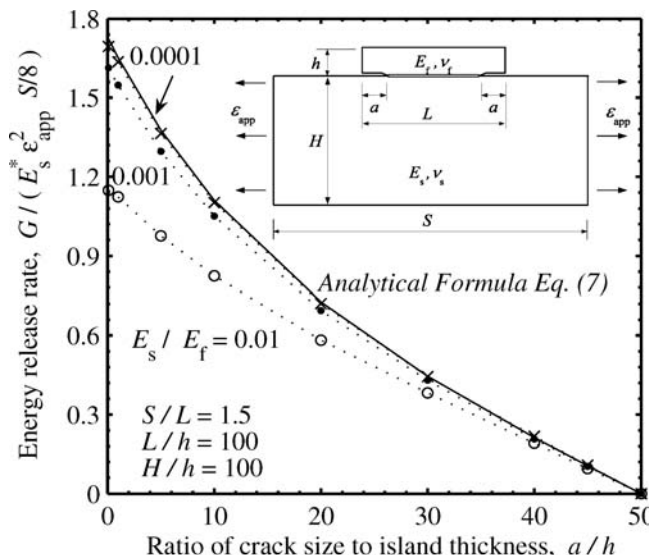


Fig. 5. FEM results compared with Eq. (7) for the debonding energy release rate of collinear periodic rigid islands on elastic solid under uniaxial tension. Equation (7) fits more accurately if the solid is more compliant or the crack is longer.

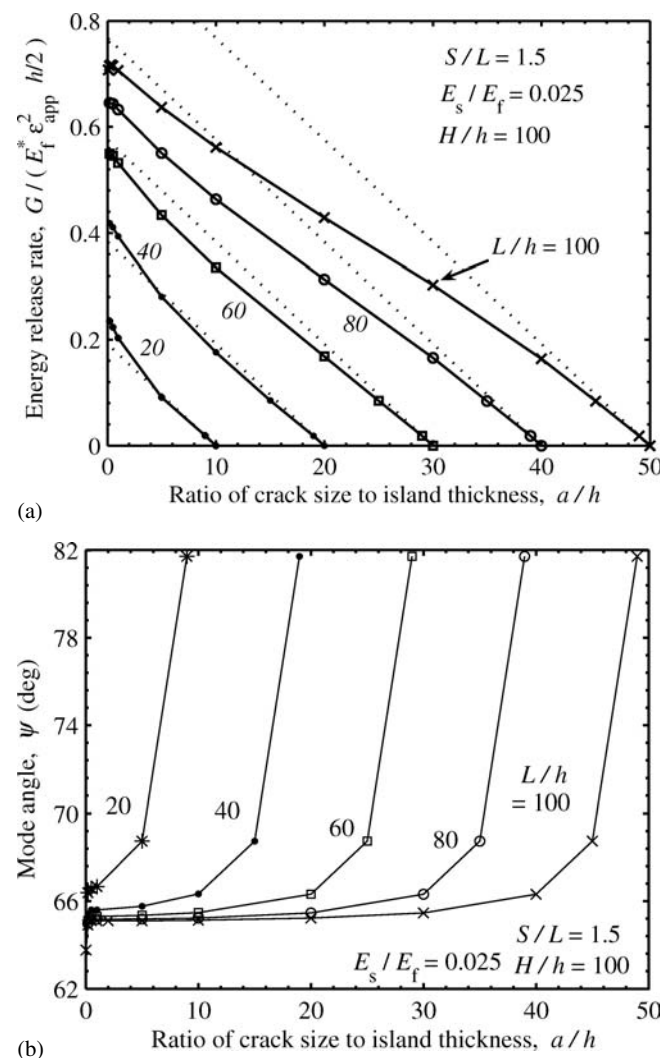


Fig. 6. (a) The energy release rate and (b) the mode angle  $\psi$ , as functions of crack size  $a/h$  for island size  $L/h$  from 20 to 100, with elastic mismatch  $E_s/E_f$ , island spacing  $S/L$  and substrate thickness  $H/h$  fixed. The energy release rates for convergent debonding (Eq. (5)) are shown by dashed lines.

#### 4. Critical island size due to interface delamination

As shown in Figs. 4–6, the energy release rate reaches a peak,  $G_{\max}$ , at a small crack length,  $a/h \sim 1$ . Figure 7 plots  $G_{\max}$  as a function of island size at several values of  $E_s/E_f$ . The peak energy release rate increases with increasing island size and substrate stiffness. The interfacial crack of any size will not grow if  $G_{\max}$  is below the interface toughness,  $\Gamma_i$ . The condition  $G_{\max} = \Gamma_i$  represents a horizontal line in Fig. 7. The intersections of this line with various curves predict the critical island sizes, below which the islands will not debond from the edges. The effect of a compliant substrate in increasing the critical island size is evident in Fig. 7. For example, take  $\Gamma_i/(E_f^* \epsilon_{app}^2 h/2) = 0.35$ , the critical island size can almost triple if the substrate stiffness reduces from  $E_s/E_f = 0.025$  to  $E_s/E_f = 0.01$ . For most interfaces,  $\Gamma_i$  also depends on the mode angle; a more precise discussion will use the mode mix angles, such as those given in Figs. 4 and 6, and use the curve  $\Gamma_i(\psi)$  obtained from experiments.

When the substrate is very compliant compared to the film, according to Fig. 5, the maximum energy release rate

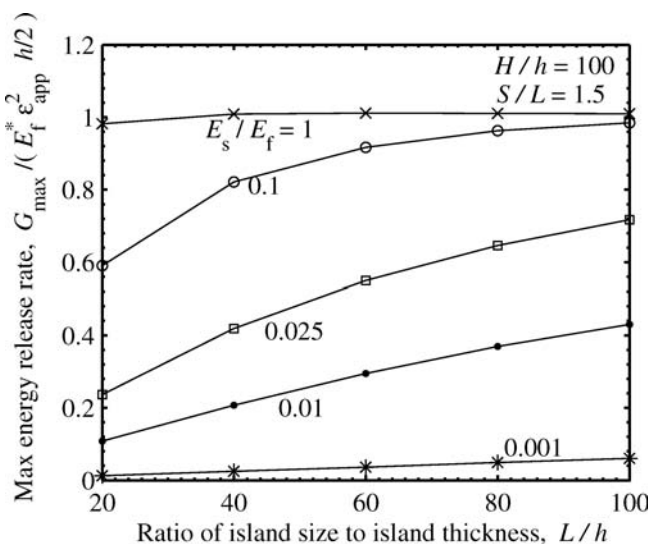


Fig. 7. Maximum energy release rate as a function of island size  $L/h$  for elastic mismatch  $E_s/E_f$  from 0.001 to 1 with  $H/h$  and  $S/L$  fixed. If we know the material properties and the interfacial toughness, this plot gives a way to determine the critical island size due to film/substrate interfacial delamination.

can be estimated by Eq. (7) with  $a = 0$ . We can set  $a$  to be zero here because with the island being rigid, the root of the  $90^\circ$  wedge can also be treated an interface crack tip. Consequently, the critical island size is given by

$$\frac{L_c}{S} = \frac{2}{\pi} \operatorname{atan} \left( \frac{8\Gamma_i}{SE_s^* \varepsilon_{app}^2} \right) \quad (10)$$

This equation is plotted in Fig. 8. The two limiting cases are readily understood. Note that  $\Gamma_i/(E_s^* \varepsilon_{app}^2)$  is a length scale. When the period is large,  $S \gg 8\Gamma_i/(E_s^* \varepsilon_{app}^2)$ , the above recovers the result of convergent debonding,

$$L_c = \frac{16\Gamma_i}{\pi E_s^* \varepsilon_{app}^2} \quad (11)$$

When the period is small,  $S \ll 8\Gamma_i/(E_s^* \varepsilon_{app}^2)$ , Eq. (10) suggests that  $L_c \rightarrow S$ . For representative parameters,  $\Gamma_i = 10 \text{ J m}^{-2}$ ,  $E_s^* = 1 \text{ MPa}$ , the length scale  $\Gamma_i/(E_s^* \varepsilon_{app}^2)$  is 10 cm when  $\varepsilon_{app} = 1\%$ , and is 1 mm when  $\varepsilon_{app} = 10\%$ .

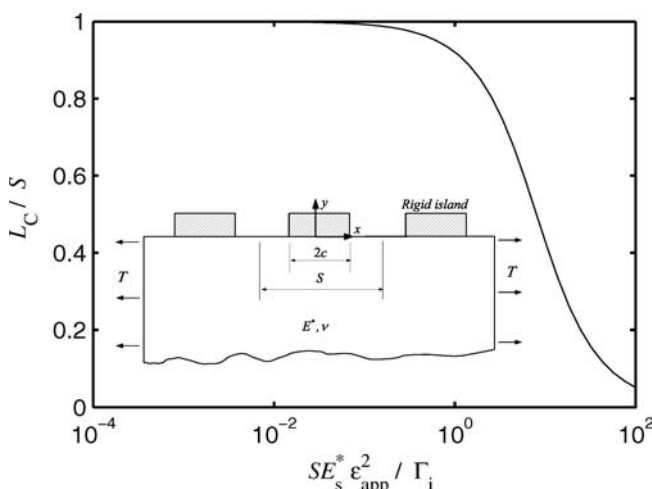


Fig. 8. The relation between the critical island size and the period (Eq. (10)). This diagram is applicable when the substrate is so compliant that the islands appear to be rigid.

## 5. Conclusions

For a structure consisting of a compliant substrate and stiff islands, when the substrate is stretched, most of the deformation is accommodated by the substrate while the islands strain little. However, flaws at the edges of the islands may cause the islands to debond. We show that the energy release rate peaks at a relatively small flaw size. If the peak energy release rate is below the interfacial toughness, no flaws will grow. Using this criterion, we show that the critical island size increases as the modulus of the substrate decreases.

The work was supported by the National Science Foundation.

## References

- [1] <http://printceoblog.wordpress.com/2007/02/08/electronic-reader-with-a-rollable-screen/>
- [2] A. Nathan, in: B.R. Chalamala (Ed.), Special Issues on Flexible Electronics Technology, Vol. 93, Proc. IEEE (2005) 1235.
- [3] G.P. Crawford: Flexible Flat Panel Displays, John Wiley & Sons, New York (2005).
- [4] A.B. Chwang, M.A. Rothman, S.Y. Mao, R.H. Hewitt, M.S. Weaver, J.A. Silvernail, K. Rajan, M. Hack, J.J. Brown, X. Chu, L. Moro, T. Krajewski, N. Rutherford: *Appl. Phys. Lett.* 83 (2003) 413.
- [5] D.W. Pashley: *Proc. R. Soc. London A* 255 (1960) 218.
- [6] H. Huang, F. Spaepen: *Acta Mater.* 48 (2000) 3261.
- [7] S.L. Chiu, J. Leu, P.S. Ho: *J. Appl. Phys.* 76 (1994) 5136.
- [8] B.E. Alaca, M.T.A. Saif, H. Sehitoglu: *Acta Mater.* 50 (2002) 1197.
- [9] D.S. Gray, J. Tien, C.S. Chen: *Adv. Mat.* 16 (2004) 393.
- [10] P.I. Hsu, M. Huang, Z. Xi, S. Wagner, Z. Suo, J.C. Sturm: *J. Appl. Phys.* 95 (2004) 705.
- [11] S. Wagner, S.P. Lacour, J. Jones, P.I. Hsu, J.C. Sturm, T. Li, Z. Suo: *Physica E* 25 (2005) 326.
- [12] R. Bhattacharya, A. Salomon, S. Wagner: *J. Electrochemical Society* 153 (2006) G259.
- [13] S.P. Lacour, S. Wagner, R.J. Narayan, T. Li, Z. Suo: *J. Appl. Phys.* 100 (2006) 014913.
- [14] H.H. Yu, M.Y. He, J.W. Hutchinson: *Acta Mater.* 49 (2001) 93.
- [15] J.W. Hutchinson, Z. Suo: *Advances in Applied Mechanics* 29 (1992) 63.
- [16] M.Y. He, A.G. Evans, J.W. Hutchinson: *Acta Mater.* 45 (1997) 3481.
- [17] H.H. Yu, J.W. Hutchinson: 423 (2003) 54.
- [18] J. Yoon, T. Li, Z. Suo: unpublished work (2006).
- [19] W.T. Koiter: *Ingenieur-Archiv* 28 (1959) 168.
- [20] J.R. Rice, G.C. Shi: *Mechanical Engineering* 87 (1965) 81.
- [21] Z. Suo: *International Journal of Solids and Structures* 25 (1989) 1133.

(Received March 23, 2007; accepted June 3, 2007)

## Bibliography

DOI 10.3139/146.101529  
 Int. J. Mat. Res. (formerly Z. Metallkd.)  
 98 (2007) 8; page 717–722  
 © Carl Hanser Verlag GmbH & Co. KG  
 ISSN 1862-5282

## Correspondence address

Zhigang Suo  
 Harvard University  
 School of Engineering and Applied Science  
 29 Oxford St., Cambridge, MA 02138, USA  
 Tel.: +1 617 495 3789  
 Fax: +1 617 496 0601  
 E-mail: suo@seas.harvard.edu

You will find the article and additional material by entering the document number MK101529 on our website at [www.ijmr.de](http://www.ijmr.de)

## Appendix. Analytical solution for periodic rigid islands on elastic substrate under uniaxial tension

This Appendix solves the linear elasticity problem of a periodic array of rigid island on a semi-infinite elastic solid (Fig. 3). We use a combination of methods in [19–21]. Under plane strain conditions, the field in the elastic solid can be represented by two standard complex potentials  $\varphi(z)$  and  $\psi(z)$ . However, another pair of commonly used potentials,  $\Phi(z)$  and  $\Omega(z)$ , defined as

$$\Phi(z) = \varphi'(z), \quad \Omega(z) = [z\varphi'(z) + \psi(z)] \quad (A1)$$

prove to be more convenient for our purpose. The stress and the displacement components are given as

$$\sigma_{xx} + \sigma_{yy} = 2[\Phi(z) + \overline{\Phi(z)}] \quad (A2)$$

$$\sigma_{yy} + i\sigma_{xy} = \overline{\Phi(z)} + \Omega(z) + (\bar{z} - z)\Phi'(z) \quad (A3)$$

$$-\frac{iE}{1+\nu} \frac{\partial}{\partial x} (u_y + iu_x) = \kappa \overline{\Phi(z)} - \Omega(z) - (\bar{z} - z)\Phi'(z) \quad (A4)$$

where  $\kappa = 3 - 4\nu$ .

Because no singularity is present inside the elastic solid, both  $\Phi(z)$  and  $\Omega(z)$  should be analytic in the half plane  $y < 0$ . The traction-free condition on the surface of the solid, in between the islands, is written as

$$\bar{\Phi}(x) + \Omega(x) = 0 \quad (A5)$$

Because  $\Omega(z)$  is analytic in the lower half plane  $y < 0$  and  $\bar{\Phi}(z)$  is analytic on the upper half plane where  $y > 0$ , we can define a function

$$f(z) = \begin{cases} \bar{\Phi}(z)y > 0 \\ -\Omega(z)y < 0 \end{cases} \quad (A6)$$

such that  $f(z)$  is analytic in the whole plane except for the rigid parts of the solid surface.

For the rigid parts of the surface, the displacement is constant. A combination of Eq. (A4) and Eq. (A6) gives that

$$\kappa f^+(x) + f^-(x) = 0 \quad (A7)$$

where  $f^+(x)$  stands for  $f(z)$  as  $z$  approaches the  $x$  axis from the upper half plane, and  $f^-(x)$  stands for  $f(z)$  as  $z$  approaches the  $x$  axis from the lower half plane.

Equation (A7) holds for  $x$  on all rigid parts of the surface, so that each rigid island serves as a branch cut for the

analytic function  $f(z)$ . The solution to Eq. (A7) is

$$f(z) = P(z) \left[ \sin \frac{\pi(z+c)}{S} \right]^{-1/2-i\varepsilon} \left[ \sin \frac{\pi(z-c)}{S} \right]^{-1/2+i\varepsilon} \quad (A8)$$

where

$$\varepsilon = -\frac{1}{2\pi} \log \kappa \quad (A9)$$

is called the oscillatory parameter which is a small number and is often reasonable to be neglected.

The function  $P(z)$  is analytic in the entire plane, satisfying the following requirements:

(a)  $\Phi(z)$  and  $\Omega(z)$  are periodic with period  $S$ ;

(b)  $\Phi(z) \rightarrow \frac{T}{4}$  and  $\Omega(z) \rightarrow -\frac{T}{4}$  for  $y \rightarrow -\infty$ ;

(c) The resultant force on each island vanishes:

$$\int_{-c}^c [f^+(x) - f^-(x)] dx = 0 \quad (A10)$$

All these three conditions can be satisfied if

$$P(z) = \frac{T}{4} \sin \frac{\pi z}{S} \quad (A11)$$

The traction at the interface a distance  $r$  from the edge of the island takes the form

$$\sigma_{yy} + i\sigma_{xy} = \frac{K r^{i\varepsilon}}{\sqrt{2\pi r}} \quad (A12)$$

The complex-valued stress intensity factor is given by

$$K = -i \frac{T}{4} \cosh(\pi\varepsilon) \sqrt{S \tan \frac{\pi c}{S}} \left( \frac{\pi}{S \sin(2\pi c/S)} \right)^{i\varepsilon} \quad (A13)$$

Note that in Eq. (A13), when  $\varepsilon = 0$ , the stress intensity is purely mode II.

The stress intensity factor relates to the energy release rate as

$$G = \frac{|K|^2}{2E^* \cosh^2(\pi\varepsilon)} \quad (A14)$$

so that

$$G = \frac{T^2 S}{8E^*} \tan \frac{\pi c}{S} \quad (A15)$$